AGU PUBLICATIONS

Geophysical Research Letters

RESEARCH LETTER
10.1002/2015GL065079

Special Section:
First Results from the MAVEN Mission to Mars

Key Points:
- We confirm that hot flow anomalies occur at Mars
- Ion perturbations are weaker than at Earth due to their relatively short lifespan
- HFAs have the potential to directly impact the topside ionosphere of Mars

Correspondence to:
G. Collinson,
glyn.a.collinson@nasa.gov

Citation:
Collinson, G., et al. (2015), A hot flow anomaly at Mars, *Geophys. Res. Lett.*, *42*, doi:10.1002/2015GL065079.

Received 30 JUN 2015
Accepted 4 AUG 2015

A hot flow anomaly at Mars

Glyn Collinson[1,2], Jasper Halekas[3], Joseph Grebowsky[1], Jack Connerney[1], David Mitchell[4], Jared Espley[1], Gina DiBraccio[1], Christian Mazelle[5,6], Jean-André Sauvaud[5,6], Andrei Fedorov[5,6], and Bruce Jakosky[7]

[1]NASA Goddard Spaceflight Center, Greenbelt, Maryland, USA, [2]Institute for Astrophysics and Computational Sciences, Catholic University of America, Washington, District of Columbia, USA, [3]Department of Physics and Astronomy, University of Iowa, Iowa City, Iowa, USA, [4]Space Sciences Laboratory, University of California, Berkeley, California, USA, [5]L'Institut de Recherche en Astrophysique et Planétologie, CNRS, Toulouse, France, [6]University Paul Sabatier, Toulouse, France, [7]Laboratory for Atmospheric and Space Physics, Boulder, Colorado, USA

Abstract One of the most important modes of planet/solar wind interaction are "foreshock transients" such as hot flow anomalies (HFAs). Here we present early observations by the NASA *Mars Atmosphere and Voltatile EvolutioN* spacecraft, confirming their presence at Mars and for the first time at an unmagnetized planet revealing the underlying ion perturbations that drive the phenomenon, finding them to be weaker than at magnetized planets. Analysis revealed the HFA to be virtually microscopic: the smallest on record at ~2200 km across and commensurate with the local proton gyroradius, resulting in a much stronger perturbation in solar wind protons than alpha particles. As at Venus, despite being physically diminutive, the HFA is still large (0.66 R_M) when compared to the relative size of the induced magnetosphere. Given the associated order of magnitude decrease in solar wind dynamic pressure (411 pPa ⇒ 70 pPa), we find that HFAs at Mars have the potential to directly impact the topside ionosphere. We thus hypothesize that the loss of a planetary magnetic dynamo left Mars far more vulnerable to the pressure pulses resulting from HFAs and related foreshock transients.

1. Introduction

There is abundant evidence that the end of the most habitable period of Martian natural history [*Masursky et al.*, 1972; *Tanaka and Kolb*, 2001; *Christensen et al.*, 2001; *Squyres et al.*, 2004; *Bishop et al.*, 2008] (the Noachian Epoch, 4.6 →3.5*Gya*) coincided with the shutdown of Mars' global magnetic field [*Acuña et al.*, 1998; *Connerney et al.*, 1999] and the transition of Mars from magnetized to an unmagnetized planet. While this timing may be purely coincidental, this fundamentally changed the solar wind obstacle from being an intrinsic magnetic field (as at Earth) to the ionosphere (as at Venus). Thus, in piecing together the natural history of Mars, it is important to understand how the solar wind interaction may also have changed.

This interaction begins in the foreshock, the region of space just upstream from a planetary bow shock. The exploration of our own foreshock has revealed it to be a highly dynamic region, wherein reside a multitude of energetic transient phenomena [see *Eastwood et al.*, 2005, and references therein]. Of all known foreshock transients perhaps the best known and most potent in terms of their known potential to cause global disruptions is the "hot flow anomaly" (HFA) [*Schwartz et al.*, 1988]. HFAs are explosive pockets of locally depleted and heated solar wind plasma that form at (and sweep across) the bow shock [*Thomsen et al.*, 1993; *Schwartz*, 1995]. At Earth, not only are they common ($\approx 2 \rightarrow 3$ per day (d^{-1}) [*Schwartz et al.*, 2000; *Facskó et al.*, 2009]) but also they can cause global scale effects on the magnetosphere and ionosphere [*Sibeck et al.*, 1998, 1999; *Jacobsen et al.*, 2009].

Figure 1 illustrates the expected conditions favoring the formation of an HFA at Mars. It begins when a tangential discontinuity (T.D.) [*Hudson*, 1970] (also referred to as a current sheet) in the interplanetary magnetic field (IMF) is brought into contact with the bow shock. The IMF, together with the antisunward flow of the solar wind across IMF lines, generates a motional electric field ($\mathbf{E} = -\mathbf{v} \times \mathbf{B}$). If these electric fields point inward on at least one side [*Thomas et al.*, 1991], then as solar wind ions are reflected at the bow shock, these fields act to focus and trap them onto the current sheet [*Burgess*, 1989], where they become heated. It is likely that heating of protons and alphas may be a result of ion-ion instabilities [*Gary*, 1991], and hybrid waves

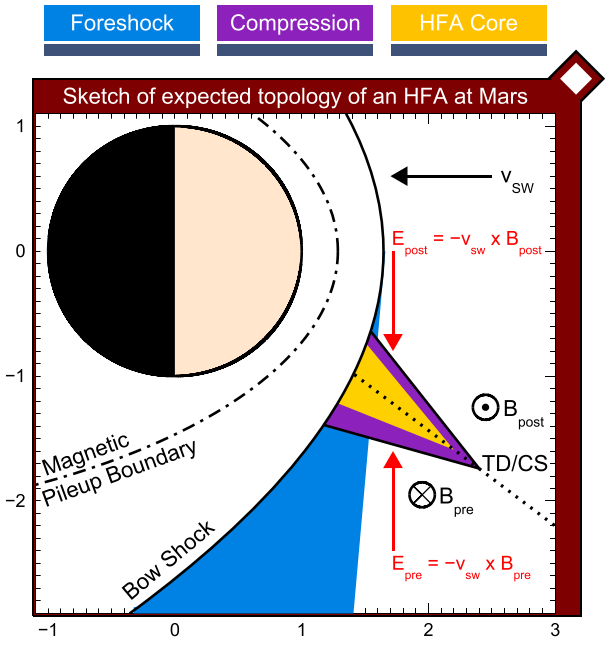

Figure 1. Schematic of the expected formation conditions and topology of a Martian HFA.

for electrons [*Zhang et al.*, 2010], although other mechanisms have been proposed. The HFA explosively expands, forming a density cavity and driving compression regions on either side resulting in an outward extension of the bow shock. An HFA thus exhibits two distinct regions: a core of hot, diffuse plasma (gold) and hot, dense bounding compression regions on either side (purple).

Recent observations by the ESA *Venus Express* [*Collinson et al.*, 2012, 2014] have found that (1) HFAs can occur at unmagnetized planets; (2) are just as common at Venus ($\approx 1.2 d^{-1}$) as at Earth; (3) although being physically smaller than their Terrestrial [*Thomsen et al.*, 1986] and Kronian [*Masters et al.*, 2008, 2009] counterparts, are very much larger when compared to the overall size of the system; and (4) occur very much closer to Venus as a result of the closer standoff distance of the bow shock. The first possible encounter with an HFA at Mars (or any other planet) was reported by *Øieroset et al.* [2001], who presented HFA-like magnetic and electron signatures from the *Mars Global Surveyor*. However, HFAs are fundamentally an ion phenomenon, and since *MGS* lacked the ion spectrometer required for identification, *Øieroset et al.* [2001] were thus appropriately cautious in their conclusions and were only able to speculate that HFAs occur at Mars. We now confirm this hypothesis, presenting an HFA at Mars encountered by the *Mars Atmosphere and Voltatile EvolutioN* (*MAVEN*) Mars Scout mission, showing magnetic observations by the MAVEN Magnetometer (MAG) [*Connerney et al.*, 2015]; ion observations by the Solar Wind Ion Analyzer (SWIA) [*Halekas et al.*, 2013]; and electron observations by the Solar Wind Electron Analyzer (SWEA).

2. Assessment of Classical HFA Formation Conditions

Figure 2 shows a map of orbit № 369 (17 December 2014) of the MAVEN Mars Scout (red), with a modeled bow shock and magnetic pileup boundary according to *Vignes et al.* [2000] (black). The coordinate system is "Mars solar orbital" where x points toward the Sun, y backward along the tangent of the orbital plane of Mars, and z completes the right-handed system pointing out of the plane of the Martian ecliptic. At 15:00 Greenwich Mean Time (GMT) (gold star), the MAVEN was in the flanks of the magnetosphere, slightly upstream of the bow shock, when an abrupt discontinuity in the IMF was blown past by the solar wind. Centered on this discontinuity was an event exhibiting all expected properties of a classical HFA. Before we discuss the event itself, we will examine the properties of this interplanetary current sheet and solar wind, and compare these conditions against the four known conditions known to be conducive for HFA formation:

F1. Motional electric fields (**E**) must point toward the interplanetary current sheet on at least one side [*Thomas et al.*, 1991; *Omidi and Sibeck*, 2007; *Schwartz et al.*, 2000] to focus solar wind ions onto the current sheet.

F2. The discontinuity must be sufficiently parallel with the Mars-Sun line so that it moves along the bow shock at a sufficiently slow speed to have an effect on solar wind particles reflected by the bow shock, such that

F3. The ratio between V_{tr}, the velocity that the discontinuity transits across the bow shock, and V_g, the angular velocity of the ions gyrating around the field lines, must be less than 1 according to equation (1) [see *Schwartz et al.*, 2000].

$$\left|\frac{V_{tr}}{V_g}\right| = \frac{\cos\theta_{cs:sw}}{2\,\cos\theta_{bs:sw}\,\sin\theta_{Bn}\,\sin\theta_{cs:bs}} \tag{1}$$

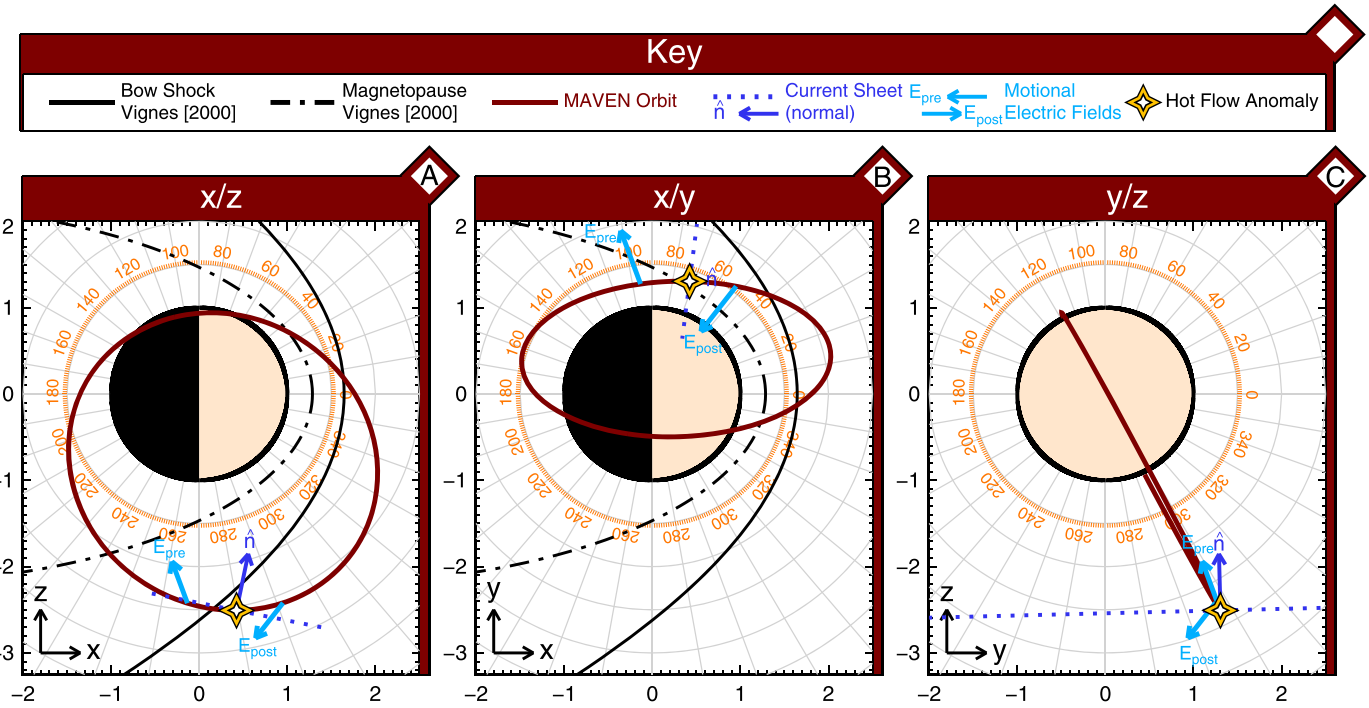

Figure 2. Map of orbit 369 of the NASA MAVEN on 17 December 2014, showing idealized model bow shock and magnetopause boundaries according to *Vignes et al.* [2000], location of the Martian HFA, and the orientation of the solar wind current sheet and motional electric fields.

F4. The solar wind velocity (V_{sw}) must be faster than average: at Earth, faster than average by ≈ 100 ⇒ 200 km/s [*Facskó et al.*, 2009, 2010] and at Venus $V_{sw} > 375$ km/s [*Collinson et al.*, 2014].

The IMF discontinuity is denoted by a dotted blue line in Figure 2, with the normal vector shown by a dark blue arrow. This was calculated by averaging the magnetic field vector before ($\bar{\mathbf{B}}_{pre}$) and after ($\bar{\mathbf{B}}_{post}$) the interplanetary current sheet, and the normal vector ($\hat{n}$, dark blue arrow) found according to equation (2) after *Hudson* [1970].

$$\hat{\mathbf{n}} = \bar{\mathbf{B}}_{pre} \times \bar{\mathbf{B}}_{post} \tag{2}$$

The results of our analysis of the current sheet are summarized in Table 1. We thus find that MAVEN was in the right place to observe an HFA, when an IMF current sheet with all the prequisite conditions conducive for HFA formation was blown past. Additionally, from the orientation of the current sheet, it would have made first contact with the bow shock on the far side of the magnetosphere; thus, the attendant HFA will be as developed as it can get at Mars, having passed over the entire dayside.

Table 1. Vector Properties of the Martian HFA and Associated IMF Current Sheet (CS), and Tests for HFA Formation Conditions

Parameter	Symbol	HFA Values	Remarks
IMF prior to CS	$\underline{\hat{B}}_{pre}$	[−0.84, 0.51, 0.18]	
IMF post CS	$\underline{\hat{B}}_{post}$	[−0.95, −0.24, 0.19]	
CS normal	$(\underline{\hat{n}})$	[0.20, −0.25, 0.98]	
Change in IMF angle	$\theta_{(\underline{\hat{B}}_{pre} \cdot \underline{\hat{B}}_{post})}$	44.53°	
Shock angle prior to CS	$\theta_{\underline{\hat{B}} \cdot \underline{\hat{n}}\,(pre)}$	117.25°	Quasi-perpendicular foreshock
Shock angle post CS	$\theta_{\underline{\hat{B}} \cdot \underline{\hat{n}}\,(post)}$	159.58°	Quasi-parallel foreshock
Electric fields		Inward toward CS	✓*F1* Focusing ions onto CS
Angle between $\underline{\hat{n}}$ and $\underline{X}_{mso}$	$\theta_{\underline{\hat{n}} \cdot \underline{\hat{x}}}$	78.51°	✓*F2* CS quasi-parallel to $\underline{X}_{mso}$
Schwartz et al. [2000] ratio	V_{tr}/V_g	0.22	✓*F3* < 1 required
Solar wind velocity	V_{sw}	450 km/s	✓*F4* Fast solar wind

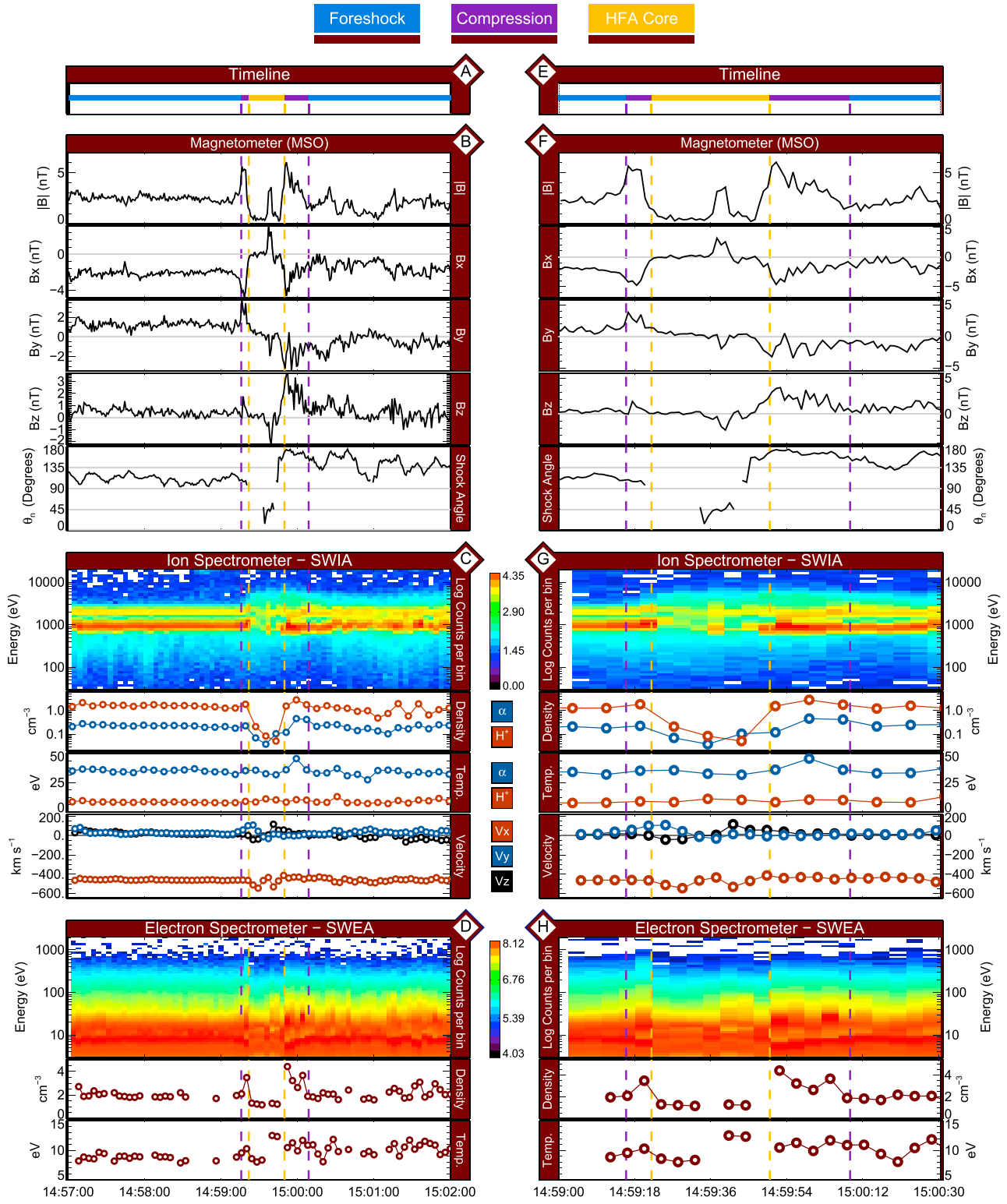

Figure 3. A hot flow anomaly at Mars. Figures 3a–3d cover the period from 14:59:00 to 15:00:30 GMT so that the field and particle perturbations can be more easily contrasted against background solar wind conditions. Figures 3a–3d show a close-up of the HFA from 14:57:00 to 15:02:00 GMT. Figure 3 is organized thus as follows: (a and e) color-coded timeline of the event. Periods when the MAVEN was in the foreshock are blue, the core of the HFA in gold, and the bounding compression regions in purple; (b and f) magnetometer data in MSO coordinates. Each component is plotted separately with θ_n, the angle that the magnetic field vector makes with the normal to the bow shock of Mars (using the *Vignes et al.* [2000] bow shock model), plotted beneath; (c and g) ion observations from SWIA, with time/energy spectrogram on top and proton density, temperature, and velocity plotted beneath; (d and h) electron observations from SWEA, with spectrogram on top and corresponding density and temperature plotted beneath.

Table 2. Plasma Moments of Separated Solar Wind Proton and Alpha Particles Before and During the Core of the HFA

Region	Time Interval (GMT)	Species	Density (cm^{-3})	Velocity (km/s) V_x	V_y	V_z	$\|V\|$	Temperature (eV)	$P_{dynamic}$ (pPa)	$P_{thermal}$ (pPa)
Foreshock	14:58:25 to 14:58:29	H^+	1.6	−441	21	−14	441	8.1	260	2.1
		α	0.22	−454	23	−13	455	37	151	0.7
HFA core	14:59:21 to 14:59:25	H^+	0.21	−467	15	−118	481	8.5	41	0.3
		α	0.07	−485	−7	−73	491	36	56	0.2
	14:59:29 to 14:59:33	H^+	0.08	−407	−19	14	407	11	11	0.1
		α	0.04	−451	6	−5	451	33	27	0.1
	14:59:37 to 14:59:41	H^+	0.05	−387	111	45	405	10	7	0.1
		α	0.10	−443	76	26	450	32	67	0.3

3. A Hot Flow Anomaly at Mars—17 December 2014

3.1. Magnetometer

Figures 3b and 3f show data from the MAVEN magnetometer. The event exhibits all magnetic signatures of an HFA: first, in the core of the event, a strong drop in ($|B|$) below ambient IMF values, with internal magnetic pulsations and, second, bounding $|B|$ enhancements associated with the bounding compressive regions. The attendant IMF discontinuity is evident from an unambiguous change in the orientation of the IMF before and after the event, with a rotation of 44.53°. This is less than the average change reported at Earth of between 60° [*Facskó et al.*, 2008] and 70° [*Schwartz*, 1995; *Facskó et al.*, 2010] and more consistent with the field rotations reported at Venus by *Collinson et al.* [2014] ($\overline{\theta}_{\underline{\hat{B}}_{pre} \cdot \underline{\hat{B}}_{post}} = 54°$). This change in IMF rotated the entire induced magnetosphere, moving MAVEN from the quasi-perpendicular to quasi-parallel foreshock. The magnetic field strength in the core of the HFA (ignoring the brief spike in the middle, which is a common feature of HFAs) is 0.5 nT, corresponding to a magnetic pressure of 0.1 pPa.

3.2. Solar Wind Ion Analyzer (SWIA)

Figures 3c and 3g show data from SWIA and represent the first time that the ion perturbations associated with an HFA have ever been resolved at an unmagnetized planet. Density and temperature are plotted separately for protons (H^+) and alpha (α) particles, based on full 3-D distributions telemetered back to Earth at 8 s resolution. Bulk velocity was calculated on board the MAVEN at 4 s resolution. Consistent with terrestrial HFAs, the core of the event was characterized by an order of magnitude decrease in proton density. An increase in ion temperature was observed but curiously was very moderate compared to HFAs at Earth and Saturn. Similarly, flow perturbations were also observed but also relatively weak when compared to its terrestrial counterparts, where HFAs have been observed to drive brief sunward (+X) flows [*Lucek et al.*, 2004]. Thus, we find the bulk ion properties measured by SWIA to be qualitatively (but not quantitatively) consistent with those reported at Earth and Saturn. Another interesting feature of the Martian HFA is that it had more of an effect on protons than alphas: Proton density falls to 3% of the foreshock value, whereas mean α density reduces on average only by 30%. Full details of the ion moments inside the core of the HFA are presented in Table 2.

3.3. Solar Wind Electron Analyzer (SWEA)

Figures 3d and 3h show electron spectrograms plus initial estimates of density and temperature. It is important to note that these moments are preliminary but are the best currently available until the spacecraft potential from the MAVEN Langmuir Probe and Waves (LPW) experiment can be utilized to remove spacecraft electrons. However, while preliminary, these initial results from Mars still represent a distinct improvement over previous investigations of HFAs at unmagnetized planets [*Collinson et al.*, 2012, 2014]. In the compression regions, SWEA observed increases in electron density comparable to that observed by SWIA, and a modest increase in electron temperature similar to the solar wind protons (Table 2). In the core, the order of magnitude decrease in plasma density (as measured independently by SWIA) makes determination of bulk plasma parameters much more challenging (as was the case at Venus in *Collinson et al.* [2012]). However, despite this, SWEA does see evidence for the known decrease in plasma density, as well as hints of increases in plasma temperature.

4. Size and Duration

Following *Thomsen et al.* [1986] and *Masters et al.* [2009], we estimated the thickness of the Martian HFA in the direction of the current sheet normal ($\hat{\mathbf{n}}$). Full details of the technique can be found in *Collinson et al.* [2014].

Applying the same technique at Mars, we found the HFA encountered by MAVEN to be virtually microscopic when compared to all others previously encountered at other planets. At 2200 km across it is the smallest HFA on record, on a par with (or possibly smaller than) the most diminutive of those observed at Venus.

Collinson et al. [2014] suggested that the smaller physical size of Cytherian HFAs may simply be a result of them not having as long to form before the current sheet entirely transits the shock, and the HFA is swept off down the magnetotail [e.g., see *Facskó et al.*, 2015]. The time taken (τ) for a current sheet to transit the bow shock from one side to the other (flank to flank) is given by equation (3).

$$\tau = \frac{2 \cdot \mathbb{BS}}{|\mathbf{V}_{sw}| \cos \theta_{\hat{\mathbf{n}}.\hat{\mathbf{x}}}} \tag{3}$$

where $\mathbb{BS}$ is the radius of the bow shock where $x = 0$. Thus, using equation (3), we may compare how long this particular current sheet (Table 1) would remain in contact with the bow shocks of the four planets where HFAs have been positively identified. Taking $\mathbb{BS}_{\text{Venus}} = 1.5{\times}10^4$ km, $\mathbb{BS}_{\text{Earth}} = 3{\times}10^5$ km, $\mathbb{BS}_{\text{Mars}} = 1.4{\times}10^4$ km, and $\mathbb{BS}_{\text{Saturn}} = 5 \times 10^6$ km, then consistent with this interpretation, to cross the bow shock from one flank to the other will take ≈3 min at Mars and Venus, ≈1 h at Earth, and ≈15 h at Saturn. Consistent with this hypothesis, we find that the specular ion distributions inside the event are more consistent with "young" or "proto" HFAs at Earth, as described by *Zhang et al.* [2010]; *Wang et al.* [2013], although as mentioned previously, the orientation of the interplanetary current sheet implies that this is as well developed as this HFA is going to get.

Another significant factor is the local proton gyroradius (r_{H^+}) of 1900 km, compared to ~500 km at Venus, ~800 km at Earth, and ~10,000 km at Saturn [*Slavin and Holzer*, 1981; *Collinson et al.*, 2014]. Given that this is comparable to the size of the HFA itself, this may also explain why alphas ($r_\alpha = 7500$ km) were less effected. Additionally, given that the total pressure was greater outside ($P_r = 411$ pPa) than inside ($\bar{P}_i = 70$ pPa), this event was collapsing [*Xiao et al.*, 2015] and may thus represent an HFA in an advanced state of decay.

5. Discussion—Potential Impact on the Martian Ionosphere

Although this HFA was physically small in absolute terms, it is none the less very large when compared to the size of the magnetosphere (0.66 Martian Radii across, where $R_M = 3{,}390$ km) [*Ball*, 1901]. *Collinson et al.* [2012, 2014] hypothesized that given this and their close proximity to the atmosphere (Figure 1), that HFAs have the potential to directly impact the ionospheres of unmagnetized planets. However, due to the poor temporal resolution of the Venus Express Ion Mass Analyzer, *Collinson et al.* [2014] was unable to observe the associated changes in dynamic pressure. For a first order approximation as to how far the location of the Martian Ionopause (R_i) might shift from its nominal radial distance (R_r) as a response to the observed pressure pulse at Mars, following *Collinson et al.* [2012] (but now armed with a much better understanding of the changes in pressure associated with such an HFA), we assume a simple static Newtonian pressure balance as below in equation (4).

$$\left(R_i - R_r\right) = -H \ln\left(\frac{P_i}{P_r}\right) \tag{4}$$

This highly simplistic model suggests that this HFA increased the height of topside ionosphere ($H \approx 40$ km) [*Withers*, 2009] by ~70 km. We therefore find that ever since the disappearance of the Martian magnetic dynamo, explosive foreshock transients such as HFAs have had the potential to directly impact the topside Martian ionosphere, and the global effects (as well as any mitigation from magnetic crustal remnants) is thus a prime topic of future investigation. While a statistical survey is required to determine their rate of occurrence, at Earth and Venus HFAs occur roughly once per day [*Collinson et al.*, 2014]. Thus, we hypothesize the following: (1) HFAs are both common and highly disruptive to the Martian system and (2) the loss of the planetary magnetic dynamo left the topside ionosphere of Mars far more vulnerable to the pressure pulses resulting from HFAs and other such common foreshock transients.

Acknowledgments
MAVEN data are available from the NASA Planetary Data System. This work was partially supported by the CNES for the part based on observations with the SWEA instrument embarked on MAVEN.

The Editor thanks two anonymous reviewers for their assistance in evaluating this paper.

References

Acuña, M. H., et al. (1998), Magnetic field and plasma observations at Mars: Initial results of the Mars Global Surveyor Mission, *Science*, *279*, 1676–1580, doi:10.1126/science.279.5357.1676.

Ball, R. S. (1901), *In the High Heavens*, Isbister and Co., London.

Bishop, J. L., et al. (2008), Phyllosilicate diversity and past aqueous activity revealed at Mawrth Vallis, Mars, *Science*, *321*, 830–833, doi:10.1126/science.1159699.

Burgess, D. (1989), On the effect of a tangential discontinuity on ions specularly reflected at an oblique shock, *J. Geophys. Res.*, *94*, 472–478.
Christensen, P. R., R. V. Morris, M. D. Lane, J. L. Bandfield, and M. C. Malin (2001), Global mapping of Martian hematite mineral deposits: Remnants of water-driven processes on early Mars, *J. Geophys. Res.*, *106*, 23,873–23,886, doi:10.1029/2000JE001415.
Collinson, G. A., et al. (2012), Hot flow anomalies at Venus, *J. Geophys. Res.*, *117*, A04204, doi:10.1029/2011JA017277.
Collinson, G. A., et al. (2014), A survey of hot flow anomalies at Venus, *J. Geophys. Res. Space Physics*, *119*, 978–991, doi:10.1002/2013JA018863.
Connerney, J., J. Espley, P. Lawton, S. Murphy, J. Odom, R. Oliversen, and D. Sheppard (2015), The MAVEN magnetic field investigation, *Space Sci. Rev.*,1–35, doi:10.1007/s11214-015-0169-4.
Connerney, J. E. P., M. H. Acuña, P. J. Wasilewski, N. F. Ness, H. Rème, C. Mazelle, D. Vignes, R. P. Lin, D. L. Mitchell, and P. A. Cloutier (1999), Magnetic lineations in the ancient crust of Mars, *Science*, *284*, 794–798, doi:10.1126/science.284.5415.794.
Eastwood, J. P., E. A. Lucek, C. Mazelle, K. Meziane, Y. Narita, J. Pickett, and R. A. Treumann (2005), The foreshock, *Space Sci. Rev.*, *118*, 41–94.
Facskó, G., K. Kecskeméty, G. Erdos, M. Tátrallyay, P. W. Daly, and I. Dandouras (2008), A statistical study of hot flow anomalies using Cluster data, *Adv. Space Res.*, *41*, 1286–1291.
Facskó, G., Z. Németh, G. Erds, A. Kis, and I. Dandouras (2009), A global study of hot flow anomalies using Cluster multi-spacecraft measurements, *Ann. Geophys.*, *27*, 2057–2076.
Facskó, G., J. G. Trotignon, I. Dandouras, E. A. Lucek, and P. W. Daly (2010), Study of hot flow anomalies using Cluster multi-spacecraft measurements, *Adva. Space Res.*, *45*, 541–552.
Facskó, G., A. Opitz, B. Lavraud, J. Luhmann, C. Russell, J.-A. Sauvaud, A. Fedorov, A. Kis, and V. Wesztergom (2015), Hot flow anomaly remnant in the far geotail, *J. Atmos. Sol. Terr. Phys.*, *124*, 39–43, doi:10.1016/j.jastp.2015.01.011.
Gary, S. P. (1991), Electromagnetic ion/ion instabilities and their consequences in space plasmas—A review, *Space Sci. Rev.*, *56*, 373–415.
Halekas, J., E. Taylor, G. Dalton, G. Johnson, D. Curtis, J. McFadden, D. Mitchell, R. Lin, and B. Jakosky (2013), The solar wind ion analyzer for MAVEN, *Space Sci. Rev.*, 1–27, doi:10.1007/s11214-013-0029-z.
Hudson, P. D. (1970), Discontinuities in an anisotropic plasma and their identification in the solar wind, *Planet. Space. Sci.*, *18*, 1611–1622.
Jacobsen, K. S., et al. (2009), THEMIS observations of extreme magnetopause motion caused by a hot flow anomaly, *J. Geophys. Res.*, *114*, A08210, doi:10.1029/2008JA013873.
Lucek, E. A., T. S. Horbury, A. Balogh, I. Dandouras, and H. Rème (2004), Cluster observations of hot flow anomalies, *J. Geophys. Res.*, *109*, A06207, doi:10.1029/2003JA010016.
Masters, A., C. S. Arridge, M. K. Dougherty, C. Bertucci, L. Billingham, S. J. Schwartz, C. M. Jackman, Z. Bebesi, A. J. Coates, and M. F. Thomsen (2008), Cassini encounters with hot flow anomaly-like phenomena at Saturn's bow shock, *Geophys. Res. Lett.*, *35*, L02202, doi:10.1029/2007GL032371.
Masters, A., et al. (2009), Hot flow anomalies at Saturn's bow shock, *J. Geophys. Res.*, *114*, A08217, doi:10.1029/2009JA014112.
Masursky, H., et al. (1972), Mariner 9 television reconnaissance of Mars and its satellites: Preliminary results, *Science*, *175*, 294–305, doi:10.1126/science.175.4019.294.
Øieroset, M., D. L. Mitchell, T. D. Phan, R. P. Lin, and M. H. Acuña (2001), Hot diamagnetic cavities upstream of the Martian bow shock, *Geophys. Res. Lett.*, *28*, 887–890.
Omidi, N., and D. G. Sibeck (2007), Formation of hot flow anomalies and solitary shocks, *J. Geophys. Res.*, *112*, A01203, doi:10.1029/2006JA011663.
Schwartz, S. J. (1995), Hot flow anomalies near the Earth's bow shock, *Adv. Space Res.*, *15*, 107–116.
Schwartz, S. J., R. L. Kessel, C. C. Brown, L. J. C. Woolliscroft, and M. W. Dunlop (1988), Active current sheets near the Earth's bow shock, *J. Geophys. Res.*, *931*, 11,295–11,310.
Schwartz, S. J., G. Paschmann, N. Sckopke, T. M. Bauer, M. Dunlop, A. N. Fazakerley, and M. F. Thomsen (2000), Conditions for the formation of hot flow anomalies at Earth's bow shock, *J. Geophys. Res.*, *105*, 12,639–12,650.
Sibeck, D. G., N. L. Borodkova, G. N. Zastenker, S. A. Romanov, and J.-A. Sauvaud (1998), Gross deformation of the dayside magnetopause, *Geophys. Res. Lett.*, *25*, 453–456.
Sibeck, D. G., et al. (1999), Comprehensive study of the magnetospheric response to a hot flow anomaly, *J. Geophys. Res.*, *104*, 4577–4594.
Slavin, J. A., and R. E. Holzer (1981), Solar wind flow about the terrestrial planets. I—Modeling bow shock position and shape, *J. Geophys. Res.*, *86*, 11,401–11,418.
Squyres, S. W., et al. (2004), In situ evidence for an ancient aqueous environment at Meridiani Planum, Mars, *Science*, *306*, 1709–1714, doi:10.1126/science.1104559.
Tanaka, K. L., and E. J. Kolb (2001), Geologic history of the polar regions of Mars based on Mars global surveyor data. I. Noachian and Hesperian periods, *Icarus*, *154*, 3–21, doi:10.1006/icar.2001.6675.
Thomas, V. A., D. Winske, M. F. Thomsen, and T. G. Onsager (1991), Hybrid simulation of the formation of a hot flow anomaly, *J. Geophys. Res.*, *961*, 11,625–11,632.
Thomsen, M. F., J. T. Gosling, S. A. Fuselier, S. J. Bame, and C. T. Russell (1986), Hot, diamagnetic cavities upstream from the Earth's bow shock, *J. Geophys. Res.*, *91*, 2961–2973.
Thomsen, M. F., V. A. Thomas, D. Winske, J. T. Gosling, M. H. Farris, and C. T. Russell (1993), Observational test of hot flow anomaly formation by the interaction of a magnetic discontinuity with the bow shock, *J. Geophys. Res.*, *98*, 15,319–15,330, doi:10.1029/93JA00792.
Vignes, D., C. Mazelle, H. Rme, M. H. Acuña, J. E. P. Connerney, R. P. Lin, D. L. Mitchell, P. Cloutier, D. H. Crider, and N. F. Ness (2000), The solar wind interaction with Mars: Locations and shapes of the bow shock and the magnetic pile-up boundary from the observations of the MAG/ER Experiment onboard Mars Global Surveyor, *Geophys. Res. Lett.*, *27*, 49–52, doi:10.1029/1999GL010703.
Wang, S., Q. Zong, and H. Zhang (2013), Hot flow anomaly formation and evolution: Cluster observations, *J. Geophys. Res. Space Physics*, *118*, 4360–4380, doi:10.1002/jgra.50424.
Withers, P. (2009), A review of observed variability in the dayside ionosphere of Mars, *Adv. Space Res.*, *44*(3), 277–307, doi:10.1016/j.asr.2009.04.027.
Xiao, T., et al. (2015), Propagation characteristics of young hot flow anomalies near the bow shock: Cluster observations, *J. Geophys. Res. Space Physics*, *120*, 4142–4154, doi:10.1002/2015JA021013.
Zhang, H., D. G. Sibeck, Q.-G. Zong, S. P. Gary, J. P. McFadden, D. Larson, K.-H. Glassmeier, and V. Angelopoulos (2010), Time history of events and macroscale interactions during substorms observations of a series of hot flow anomaly events, *J. Geophys. Res.*, *115*, A12235, doi:10.1029/2009JA015180.